Coherent and incoherent giant dipole resonance γ-ray emission induced by heavy ion collisions: Study of the $^{40}Ca+^{48}Ca$ system by means of the constrained molecular dynamics model

Massimo Papa,[1,*] Antonio Bonanno,[2] Francesca Amorini,[3] Aldo Bonasera,[3] Giuseppe Cardella,[1] Alessia Di Pietro,[3] Pier Paolo Figuera,[3] Toshiki Maruyama,[4] Giuseppe Pappalardo,[2] Francesca Rizzo,[2] and Salvatore Tudisco[3]

[1]*Istituto Nazionale Fisica Nucleare-Sezione di Catania, Corso Italia 57, 95129 Catania, Italy*

[2]*Dipartimento di Fisica e Astronomia, Universitá di Catania, Via Santa Sofia 64, 95123 Catania, Italy*

[3]*Istituto Nazionale Fisica Nucleare-Laboratorio Nazionale del Sud, Via Santa Sofia 44, 95123 Catania, Italy*

[4]*Advanced Science Research Center, Japan Atomic Energy Research Institute, Tokai, Ibaraki 319-1195, Japan*

(Received 31 July 2002; revised manuscript received 13 March 2003; published 9 September 2003)

Coherent and incoherent dipolar γ-ray emission is studied in a fully dynamical approach by means of the constrained molecular dynamics model. The study is focused on the system $^{40}Ca+^{48}Ca$ for which recently experimental data have been collected at 25 MeV/nucleon. The approach allows us to explain the experimental results in a self-consistent way without using statistical or hybrid models. Moreover, calculations performed at higher energy show interesting correlations between the fragment formation process, the degree of collectivity, and the coherence degree of the γ-ray emission process.

DOI: 10.1103/PhysRevC.68.034606 PACS number(s): 24.10.−i, 24.60.−k, 24.30.Cz, 21.60.−n

I. INTRODUCTION

During the past 20 years, giant dipole resonance (GDR) γ-ray emission induced by heavy ion collisions has raised a large interest especially concerning the study of GDR properties in hot and deformed fissioning nuclei [1–4] up to the critical temperature [5–11], and more recently concerning the pre-equilibrium emission (see, for example, Refs. [12–14]).

In several experiments around 8–10 MeV/nucleon [12,14–19], it was pointed out that the γ-ray yield is increased with respect to statistical calculations in the region around 10 MeV, for systems with mass less than 150 and having a pronounced difference in the charge/mass ratio between projectile and target. This enhancement was ascribed, according to various theoretical arguments, to preequilibrium effects (see, for example, Refs. [14,20–24]). In particular, in Ref. [14] this effect was related to the charge/mass equilibration process which starts with the overlap of the two nuclei. In that work the study was performed for fusion, incomplete fusion, and deep inelastic processes using a semiclassical theory based on the Boltzmann-Nordheim-Viasov (BNV) approach [25]. Moreover, for midperipheral reactions it was shown that the so-called ''molecular dipole component'' is the most important one [14]. It reveals in fact the collective character of the charge and mass exchange between the two partners. In the same work a prediction of the preequilibrium yield in absolute units has also been given. The prediction was obtained in the semiclassical approximation, by applying the Larmor formula to the dipole, obtaining a satisfactory agreement with the data [12,16,17]. A comparison with the statistical model was also performed based on the local time equilibrium hypothesis. Using the same approach, the data of Ref. [18] have also been recently discussed in Ref. [24].

More recently, these kind of studies have been performed on the systems $^{40}Ca+^{48}Ca$ and $^{40}Ca+^{46}Ti$ at 25 MeV/nucleon [11]. The second system has been taken as a reference system: in fact, for the $^{40}Ca+^{46}Ti$ system this preequilibrium effect is negligible because of the very similar charge/mass ratio between projectile and target.

So far the dynamical studies on this subject have been performed using a semiclassical mean field theory. In Ref. [26] it has been noted that, especially in the Fermi energy domain, the role played by the fluctuations around the mean values should be investigated in a consistent way using a dynamical approach.

In the present work we will develop the study on the above subjects with the constrained molecular dynamics (CoMD) model [27]. The model takes into account the effect of the fermionic nature of the nuclear many-body system by constraining the phase space to fulfill at each time step the Pauli principle. In the CoMD model the ''ground state'' configuration, obtained with a ''cooling'' procedure coupled with the constraint, is a very stable configuration (up to a time of the order of 1500 fm/c). In contrast to other molecular dynamics approaches, the average effective kinetic energy of a nucleon, for these configurations, is comparable with the value estimated in the Thomas-Fermi model (around 20 MeV/nucleon). The CoMD model has been successfully applied to the experimental fragment charge distribution obtained in the collisions $^{40}Ca+^{40}Ca$, $^{197}Au+^{197}Au$ [27,28], and in the $^{112,124}Sn+^{58,64}Ni$ systems at 35 MeV/nucleon [29,30]. The effective interaction has been taken as a Skyrme-I force plus a surface term and a density independent symmetry interaction. The Coulomb interaction is also included.

To present the main line of investigation suggested by this dynamical approach, in Fig. 1 we show the time derivative of the total dipole, along the beam direction V_Z, as function of time. In the figure we show three typical events representing the system $^{40}Ca+^{48}Ca$ at 25 MeV/nucleon in a central collision. For the present study we have generated all the events by initializing the colliding system with identical macro-

*Email address: papa@ct.infn.it

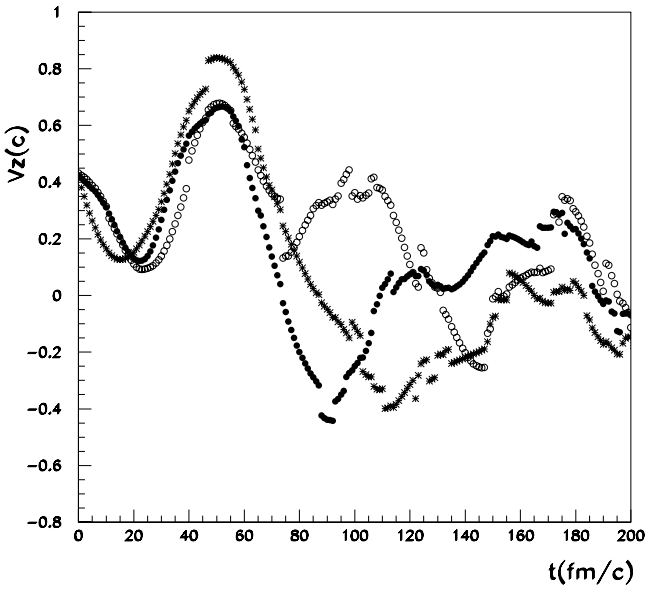

FIG. 1. Time derivative of the total dipole along the beam directions as function of time calculated by means of the CoMD model. The three different symbols are related to three different microscopic realizations of the ^{40}Ca+^{48}Ca system at 25 MeV/nucleon and for an impact parameter $b=0$ fm.

scopic initial conditions (same impact parameter, same total spin, same incident energy). As we will discuss in detail, the time derivative of these quantities are directly linked with the γ-ray emitted power. The three curves, plotted with different symbols, show very similar behavior in the first 100 fm/c. This similarity determines an ensemble average different from zero. The average shows quasiperiodicity and gives rise to the so-called coherent contribution to the collective neutron-proton motion. It is also strongly related to the charge/mass asymmetry differences in the entrance channel (see Appendix A). Because of the coherence, the related GDR mode acquires a macroscopic behavior.

After some time the three signals lose their phase relations, even though they are always characterized by an oscillating behavior. This on the one hand will damp the coherent mode, but on the other hand will give rise to the so-called fluctuating (with respect to the ensemble average) or incoherent collective motion. This kind of behavior is able to mimic the statistical emission of a hot compound system.

Finally, all the signals at different times show discontinuities produced by the nucleon-nucleon scattering process. This microscopic incoherent motion (or noncollective) will contribute to the GDR damping. It will also determine the high energy spectral properties of the emitted radiation or the so-called bremsstrahlung contribution.

All these contributions and their interplay are interesting for several reasons. In fact, we have the following.

(i) The strength connected to the fluctuating or incoherent dipolar collective excitations should correspond, for a fully equilibrated system, to the strength predicted by the statistical compound nucleus theory included in the statistical code CASCADE [31]. In a rather general way, we can expect (see Ref. [26]) that this contribution also shows a preequilibrium stage. On the other hand we will show that the coherent oscillations give the strongest contributions during the very initial stage of the interaction. During this stage the intermediate system is strongly deformed, and therefore the coherent contribution gives the possibility to investigate these rather short lived and exotic shapes.

(ii) Both the dynamical stage and the onset of fluctuations on the collective coordinate can be affected by the formation of fragments during the multifragmentation of a hot source induced by the heavy ion collision. This effect needs a fully dynamical study of the many-body problem including the reaction dynamics. In general, it cannot be investigated by means of statistical models or hybrid models. These last models are essentially statistical models in which some parameters are supposed to be time dependent quantities evaluated through some dynamical approach. In this case a local time equilibrium hypothesis is necessary.

(iii) Other interesting examples of interplay of coherent and incoherent processes have been studied in nuclear physics. One of these is the phenomenon of the partial coherent rotation of the double nuclear system revealed through the study of the fluctuations in the excitation function of deep inelastic processes [32,33]. The gradual loss of coherence of the process, related to the dissipative properties of the system, can be connected to the transition from ordered to chaotic behavior of the system, and the coherent part mimics the classical rotation of the system. From a quantum mechanical point of view, it is related to the excitation of special states of the systems described through a strong coherence in the partial waves describing the process. The same can happen to the proton-neutron relative motion. In this case these special coherent states manifest themselves through the coherent γ-ray preequilibrium emission.

In the following we will try to discuss these different aspects by comparing the model calculations with experimental results for central collisions [11]. In particular in Sec. II we will illustrate the experimental results obtained for the systems ^{40}Ca+^{48}Ca and ^{40}Ca+^{46}Ti [11] at 25 MeV/nucleon in central collisions. A detailed description on the selection criteria used for the data analysis will also be given. In Sec. III we show the CoMD calculations related to the coherent emission and we compare them with the experimental results. In Sec. IV we give the results for the incoherent or fluctuating collective mode as obtained from CoMD calculations. A comparison with calculations based on the Langevin approach is also discussed. The Langevin approach, which we briefly discuss in Appendix A, will allow us to make a comparison between the results obtained through our self-consistent microscopic approach and a well-established simple dynamical theory in which some preequilibrium effects can be included.

Finally, in Sec. V we will show some results for central collisions calculations at higher energies for which multifragmentation of the primary hot source is obtained. The degree of coherence and the degree of collectivity for the dipolar mode is studied as function of the bombarding energy.

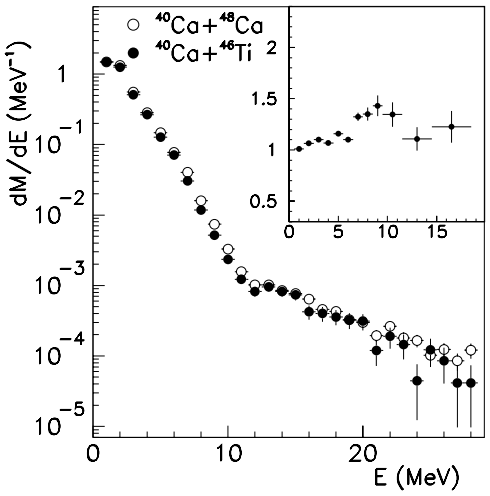

FIG. 2. Experimental γ-ray spectra detected at 90° obtained for the collision ^{40}Ca+^{48}Ca and ^{40}Ca+^{46}Ti at 25 MeV/nucleon, in coincidence with evaporation residues. The heavy ion selection is obtained with the condition on the scatter plot E_{lab} versus rise time (expressed in arbitrary units) shown in Fig. 3. In the inset the ratio between the yields is shown.

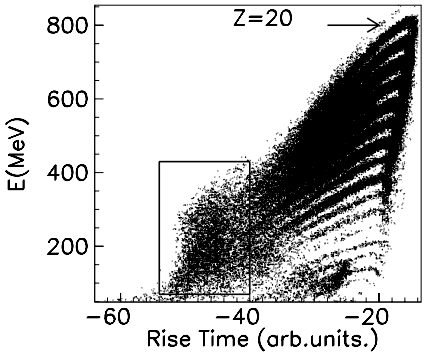

FIG. 3. Scatter plot showing the laboratory kinetic energy versus rise time (arbitrary units) of the charged particles stopped in the silicon detectors for the collision ^{40}Ca+^{48}Ca at 25 MeV/nucleon (data from Ref. [11]). The contour in the scatter plot represents the correlated condition on the energy and rise time used in the data analysis to select the heavy residues.

II. THE EXPERIMENTAL DATA

In Fig. 2 we show the experimental γ-ray spectra detected at 90° with respect to the beam direction for the collisions ^{40}Ca+^{48}Ca and ^{40}Ca+^{46}Ti [11] at 25 MeV/nucleon in coincidence with evaporation residues. In the inset we also show the relative ratios. The vertical and horizontal bars indicate the errors related to the counting statistics and to the systematic errors on the energy. The latter ones are mainly due to the uncertainty on the energy calibration.

In the inset it is evident that there is an extra yield of the order of 50% around 10 MeV. The process has been selected for both systems by measuring the γ-ray yield in coincidence with events producing heavy charged ions. The evaporation residues have been selected by putting a contour on the energy ''rise-time'' scatter plot for particles stopped inside the forward silicon detector (300 μm thick). The rise-time is expressed in arbitrary units. This detector covers the laboratory angular range of 3°–6°. An example of such selection condition is displayed in Fig. 3 for ^{40}Ca+^{48}Ca at 25 MeV/nucleon. In the figure the scatter plot is shown with the contour. These limits mainly include slow heavy fragments produced in central collisions. This is confirmed also by the measured intensity of the bremsstrahlung yield which, for the events populating the selected region, displays a yield at least two times higher than the yield collected for particles outside the chosen contour. An analysis based on Ref. [34] gives an average impact parameter contributing to the process equal of about 3 fm (corresponding to an incident angular momentum of about 71$\hbar$).

In Ref. [11] the global features of γ-ray yields have been described by means of a standard analysis using CASCADE calculations. In this case it was supposed, according to the experimental results of Ref. [35], that a hot source is formed with an estimated mass of about 62 and an excitation energy of about 335 MeV and 354 MeV for ^{46}Ti and ^{48}Ca targets, respectively. The estimated average angular momentum of the source was 29$\hbar$.

In the following sections we will describe the main features of the γ-ray yields using the dynamical approach based on the CoMD model. In particular, in Ref. [11] the study performed did not include the evident low energy γ-ray extra yield for the ^{40}Ca+^{48}Ca system as shown in Fig. 2.

To perform this kind of study we have to determine an impact parameter window for which the same processes, essentially incomplete fusion, are selected in our CoMD model calculations as in the experimental data. In Fig. 4 we show the comparison between the experimental energy spectrum of the charged particles, selected by the contour in Fig. 3 (full circles), and the theoretical prediction (empty circles). The uncertainty on the energy of the detected fragments is less than 10%. It arises principally from the thickness of the dead layer and from the pulse defect.

Theoretical predictions have been obtained by running several thousands of CoMD events with a triangular impact parameter distribution up to $b_{max} \simeq 8.5$ fm. The dynamical calculations have been followed up to 800 fm/c. At this time the average excitation energy of the hot sources is about 3 MeV/nucleon. After this first stage a second step, based on GEMINI code [36], has been applied to the hot fregments to simulate the statistical evaporation of the excited fragments.

From the total number of generated events, we have considered only those which satisfy the conditions imposed by the experimental filter. These conditions include the laboratory angle range (3°–6°) and the energy thresholds depending on the atomic number of the detected fragments according to the contour shown in Fig. 3. The calculated spectrum reproduces well the experimental one. The error bars are related to the statistics of the simulations. Evaporation residues with charge Z less than 23 mainly determine the maximum in the energy spectrum of the theoretical distribution.

In the inset of the figure the related impact parameter distribution computed with the events selected with the experimental constraints is also shown. For lower impact parameters the reduction of the detection probability is determined by the kinematical conditions selected by the

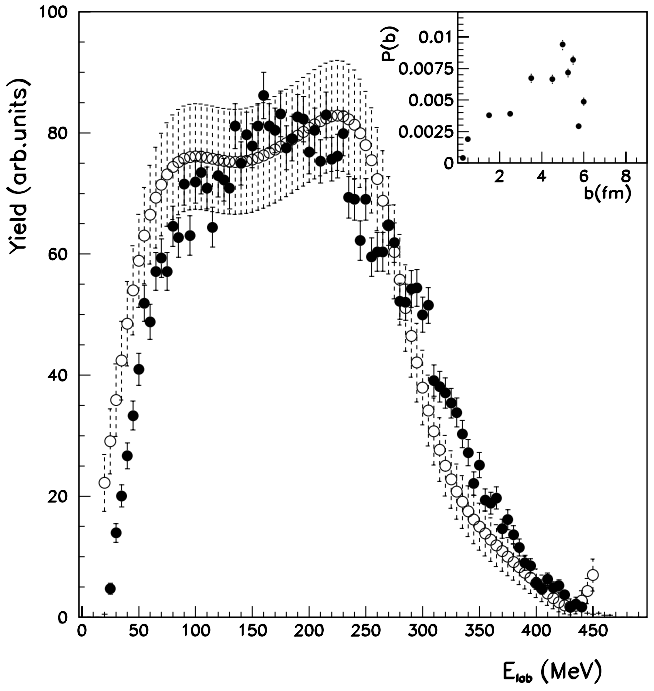

FIG. 4. Experimental (full circles) and calculated (empty circles) laboratory energy spectra for the incomplete-fusion heavy residues selected by the contour in Fig. 3. In the inset the related impact parameter window determined through CoMD calculation is also shown. The probability distribution has been evaluated by considering large-scale calculations with different impact parameters distributed according to a triangular distribution up to $b_{max}=8.5$ fm. The error bars indicate the uncertainty related to the statistics of the event collection.

experimental angular range. Starting from $b \simeq 4$ fm, the strong reduction of the probability distribution yield is also produced by the onset of binary processes which are strongly suppressed by the contour in Fig. 3. The impact parameter average value is about 4 fm corresponding to an incident angular momentum of about $90\hbar$. This estimated window of the contributing impact parameters or total angular momentum will be used for our further calculations on the γ-ray probability emission.

III. THE COHERENT CONTRIBUTION

As it was observed in the preceding section the ^{40}Ca $+^{48}$Ca system shows an extra yield in the γ-ray spectrum respect to ^{40}Ca$+^{46}$Ti. In particular at 11 MeV the extra yield is of the order of 35%. At the same energy the observed multiplicity (see Fig. 2) corresponds to a maximum of about 10^{-3} MeV^{-1} for the selected processes.

In the following section we will illustrate the calculations based on the CoMD approach to explain these experimental observations as a result of the dynamical effect arising from the different charge/mass ratios between the two systems.

Before showing the results of the nucleus-nucleus collision on the dipolar γ-ray emission, we briefly comment the properties of the ''ground state'' configurations for the impinging nuclei, as obtained from our calculations. As an example in Fig. 5 we show the root mean square radius of ^{48}Ca as function of time [panel (a)] and the energy distribution of the GDR dipolar mode [panel (b)] obtained from a small relative displacements of the neutron and proton spheres. The energy is peaked around 16–17 MeV, about 15% lower than the value predicted according to the droplet model in Ref. [37]. The binding energy of the ground state configuration is about 8.2 MeV/nucleon. Similar results have been obtained within a few percent, for the ^{40}Ca and ^{46}Ti systems.

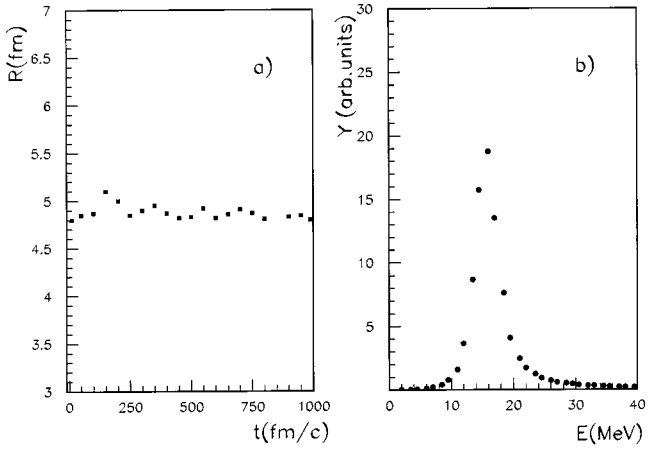

FIG. 5. (a) Root mean square radius for a typical ground state configuration of the ^{48}Ca nucleus produced in the CoMD approach. (b) The related energy distribution of the GDR mode. The uncertainty on the energy axis of every point is ± 650 keV (see the text).

A. Coherent emission in the ^{40}Ca+^{48}Ca system

Several hundreds of initial configurations have been generated with the above average behavior within 2% of uncertainty. In Fig. 6 we show, as an example, the results for the ^{40}Ca+^{48}Ca collision at 25 MeV/nucleon for $b=3.5$ fm. In the left panels are given, in units of the elementary charge, the ensemble average values for the time derivative of the total dipole $\vec{V}=\Sigma_{i=1,Z}(\overline{d\vec{r}_i/dt})$ along the impact parameter direction X and along the beam direction Z as function of the time t in fm/c. The bar in the previous expression indicates the ensemble average. We note that the coherent oscillations survive up to the first 170 fm/c.

In the right panel the γ-ray emission probability for energy unit is shown. It was calculated by means of the Fourier transform of the time derivative of the k components X and Z of $\vec{V}$ according to the following relations:

$$\frac{dP}{dE}=\frac{4}{6\pi}\frac{e^2}{E\hbar c}\left|\overline{\frac{dV_k}{dt}}(E)\right|^2, \tag{1}$$

$$\overline{\frac{dV_k}{dt}}(E)=\int_0^{\infty}\overline{\frac{dV_k}{dt}}(t)e^{i(Et/\hbar c)}dt. \tag{2}$$

dP/dE has to be interpreted as the average number of γ rays emitted for energy unit. The evaluation of emitted power is therefore performed by means of classical electrodynamics in which radiative effects on the nucleon dynamics

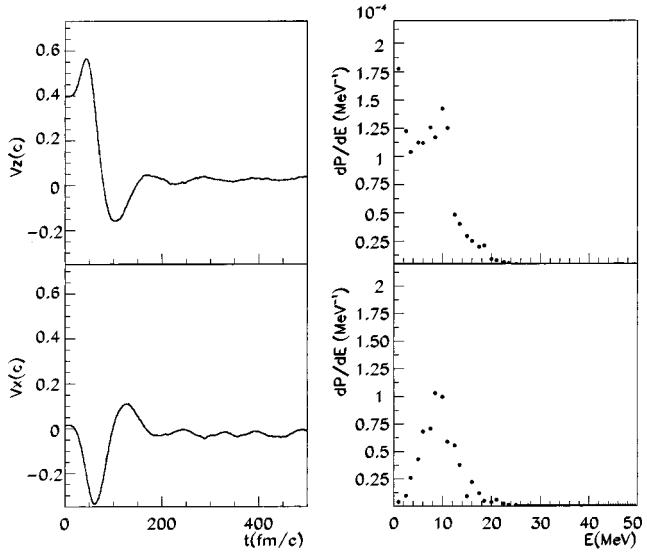

FIG. 6. On the right side are shown the time derivative of the average total dipole along the beam direction V_Z and along the impact-parameter direction V_X as function of time, for the ^{40}Ca $+^{48}$Ca system at 25 MeV/nucleon and $b=3.5$ fm. On the left side are shown the related γ-ray yield distributions. The uncertainties on the *y*-axis related to the ensemble averages are of the order of 2%. The energy axis of every point is undetermined within ± 650 keV.

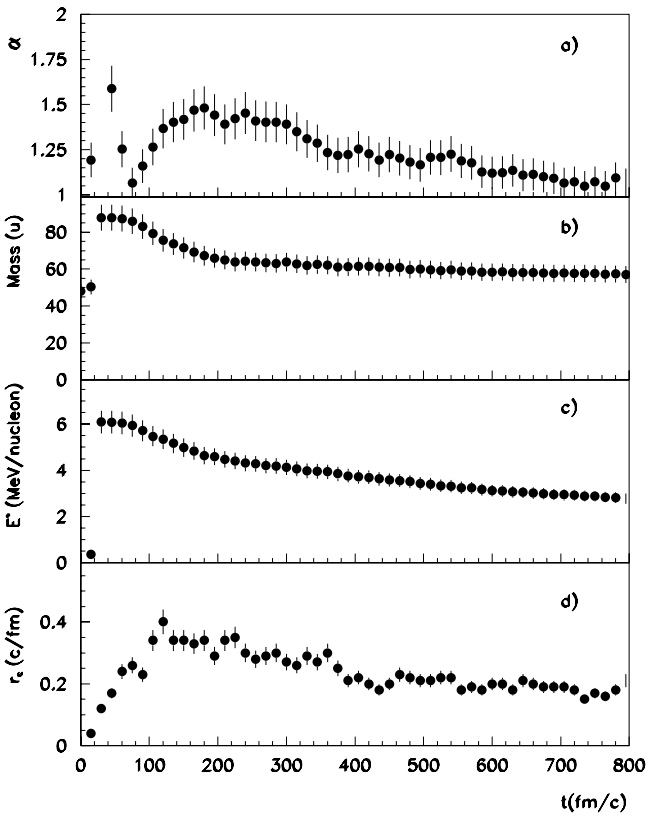

FIG. 7. Time evolution for the ^{40}Ca+^{48}Ca system at 25 MeV/nucleon and $b=3.5$ fm of (a) the ratio α between the length of the major axes and the average length of the other two axis characterizing the shape of the intermediate system, (b) calculated average mass of the biggest fragment, (c) related average excitation energy, and (d) the average collision rate. The error bars indicate the uncertainty related to the statistics of the simulation.

are considered negligible. Because of the finite time interval effect, the uncertainty related to the energy is ± 650 keV in all the calculated γ-ray spectra.

From the same calculations one finds that the $\overline{V_y}$ component is not excited through this mechanism since, on average, the displacement in the phase space along the *Y* direction of the neutron and proton sphere is zero [see Eqs. (3.4) and (3.5) in Ref. [14]]. This in principle can produce strong anisotropy not only related to the deformation of the compound system [26].

The total strength shows a dependence on the impact parameter. The maximum is obtained for the impact parameters in the range $b=2-5$ fm. The intensity at the maximum for *b* around 4 fm, which represents the centroid of the selected *b* window is about 2×10^{-4} MeV^{-1}. This value is in good agreement with the experimental one at 11 MeV.

Concerning the spectral properties of the coherent emitted power we note a rather narrow width (about 6 MeV) and a low resonant energy (about 10 MeV). This is consistent with a rather low collision rate r_c (even if rapidly increasing) in the first moments of the collision and with the large deformation and mass of the total system during the preequilibrium stage. These effects are shown in Fig. 7 where we display some results for the collision under study at $b=3.5$ fm. The error bars are related to the statistics of the simulation. In particular in panel (a) we display, as function of time, the ratio α between the length of the major axes and the average length of the other two axis characterizing the triaxial shape of the biggest fragment. Evident deformation effects are present during the first <300 fm/c in which the coherent emission is prominent. An analysis performed on the shape of the deformed source gives a ratio between the sphericity *S* and coplanarity *C* parameters corresponding to triaxial shapes which can be well approximated by a prolate ellipsoid ($S/C\simeq1$). Moreover, the direction of the total angular momentum is perpendicular to the major axis.

In panel (b) of the same figure we show the average mass of the biggest fragment. The corresponding excitation energy E^* per nucleon is shown in panel (c). One observes a rapid change of the mass for the largest fragment during the first 200 fm/c. The residue is formed after this time interval when the coherent (see Fig. 6) oscillation is almost totally damped. It is still possible to note that notwithstanding the rather high excitation energy in the first 200 fm/c, the nucleon-nucleon collision rate, which is shown in panel (d), is lower than the maximum value reached after about 120 fm/c. This is due to the gradual opening of the phase space available for the unblocked collisions and explain the rather small width of the preequilibrium coherent γ-ray emission, despite the high excitation energy of the intermediate system. For this value of the impact parameter, we have also calculated the total angular momentum of the heavy residues produced after 200 fm/c. It results about $50\hbar$ which is 25% higher than the prediction for the critical angular momentum according to the liquid drop model [38]. At 200 fm/c the average excitation energy of the hot source is about 5 MeV/nucleon in agreement, within 15%, with the

analysis performed in Ref. [11].

The investigation concerning the average shapes, angular momentum, and excitation energy has been performed also for the ^{40}Ca+^{46}Ti system. For this system we have obtained result similar to the previous ones within 10%. The remarkable difference between the two systems is instead obtained for the coherent emission which, for the ^{40}Ca+^{46}Ti system, is at least a factor of 20 weaker with respect to the ^{40}Ca $+^{48}$Ca case.

On the basis of the results shown in Fig. 7, we finally note that the initial dipolar coherent emission can be also used to investigate on other dynamical properties, for example, the degree of deformation, the shapes, and collision rate of the hot compound system during the short time interval before the fragment formation process.

IV. THE INCOHERENT CONTRIBUTION

In the preceding section we have illustrated the results for the coherent γ-ray emission that represents one of the preequilibrium effects. As discussed in the introduction, the incoherent collective emission (or statistical) can also show preequilibrium effects; therefore a dynamical description is necessary. Moreover, the experimental results presented in Sec. II show the coherent effect (see Fig. 2) by the ratio of the yields obtained for very similar total systems. This represents the relative contribution between the coherent plus incoherent emission in the ^{40}Ca+^{48}Ca system and the essentially incoherent or statistical emission produced in ^{40}Ca $+^{46}$Ti system. Therefore, to describe in a consistent way the experimental observations on the coherent emission, we also have to describe the incoherent contribution with the same theoretical approach.

This subject, if treated with a fully dynamical approach, can reveal considerable difficulties. One of these is the time necessary to describe the incoherent emission. The statistical emission can in fact go on up to several thousands of fm/c. Another difficulty is the definition of temperature. This definition is encountered when a necessary comparison of our model description is done with statistical model prediction over long times. Determining a time interval after which the thermal equilibrium is reached by our system solves the first problem. To obtain this, with our Fourier analysis, it will be enough to follow the dynamical evolution up to 1000 fm/c. We have solved the second problem by comparing our predictions with a simple and well-known dynamical model based on the Langevin equation (see Appendix A) in which the temperature characterizes the behavior of the stochastic forces acting on the total dipole.

A. Incoherent emission in the ^{40}Ca+^{48}Ca system at 25 MeV/nucleon

For the same set of events for which we have deduced the average properties of the generic dipolar component, we can compute the power connected to the fluctuating or incoherent one. In particular, the second time derivative of the incoherent dipolar signals is given by the following relation: $dV^i_{k,f}/dt=(dV^i_k/dt)-[\overline{dV_k(t)/dt}]$ [see also Eq. (A2)].

Through a Fourier transform it is possible to calculate the spectrum of the incoherent emission during the first 1000 fm/c in which the dynamical evolution has been followed. In particular the quantity

$$\frac{dP}{dE}=\frac{4}{6\pi}\frac{e^2}{E\hbar c}\sum_k\overline{\left|\frac{dV^i_{k,f}}{dt}(E)\right|^2}, \tag{3}$$

representing the number of γ rays per energy unit emitted through the incoherent mechanisms has been evaluated by means of the Fourier components of the accelerations $dV^i_{k,f}(E)/dt$.

We note that the Parseval theorem links Eq. (3) to Eq. (A9) according to the following relation:

$$\int_0^\infty\frac{d\epsilon}{dt}dt=\int_0^\infty E\frac{dP}{dE}dE, \tag{4}$$

where $d\epsilon/dt$ is the average power emitted at the time t.

This relation holds even if the numerical calculation of the Fourier transform is performed in finite time intervals t_m (in our case 1000 fm/c) and it gives a useful normalization rule. The results of the described calculations are shown in Fig. 8 for the system under study at 25 MeV/nucleon and $b=0$ fm. In panel (a) the power emitted as function of time (collective plus bremsstrahlung contributions) relative to the Z component is shown as empty circles, whereas the stars and the full line represent predictions according to the standard statistical model calculations or Langevin calculations (see the Appendixes). The full circles represent the collective contribution as obtained by CoMD calculations. We have also verified that for the fluctuating parts the signals of the different components show correlation coefficients less than 5%, therefore within the uncertainty of the calculations, we can assume that they are uncorrelated. This is also consistent with the sum performed in Eq. (3). In this way, for the comparison, the one-dimensional results of the Langevin approach shown in Appendix A can be applied for each component.

In panel (b) we show the average multiplicity distribution dP/dE connected to the incoherent collective process along the Z axis (full circles) and those connected to the coherent process (empty circles). Finally, in panel (c) the average masses correspond to the two largest fragments and, in panel (d), the related excitation energies as a function of time are shown. The errors on the displayed quantities are less than 2% and are due to the statistics of the simulation.

The average multiplicity distribution shown in Fig. 8(b) is peaked around 15 MeV. This indicates that the evaluated incoherent contribution has essentially a collective character. We will comment on this aspect with more details in the following sections. Within the uncertainty of the Fourier analysis (about 1.3 MeV), the energy centroid displays a slightly smaller value with respect to the value obtained in the frame of the liquid drop model applied to the total system [37]. This is due both to the effective interaction used, which can also generate a small underestimation of the centroid value (see Sec. I), and to deformation and expansion effects

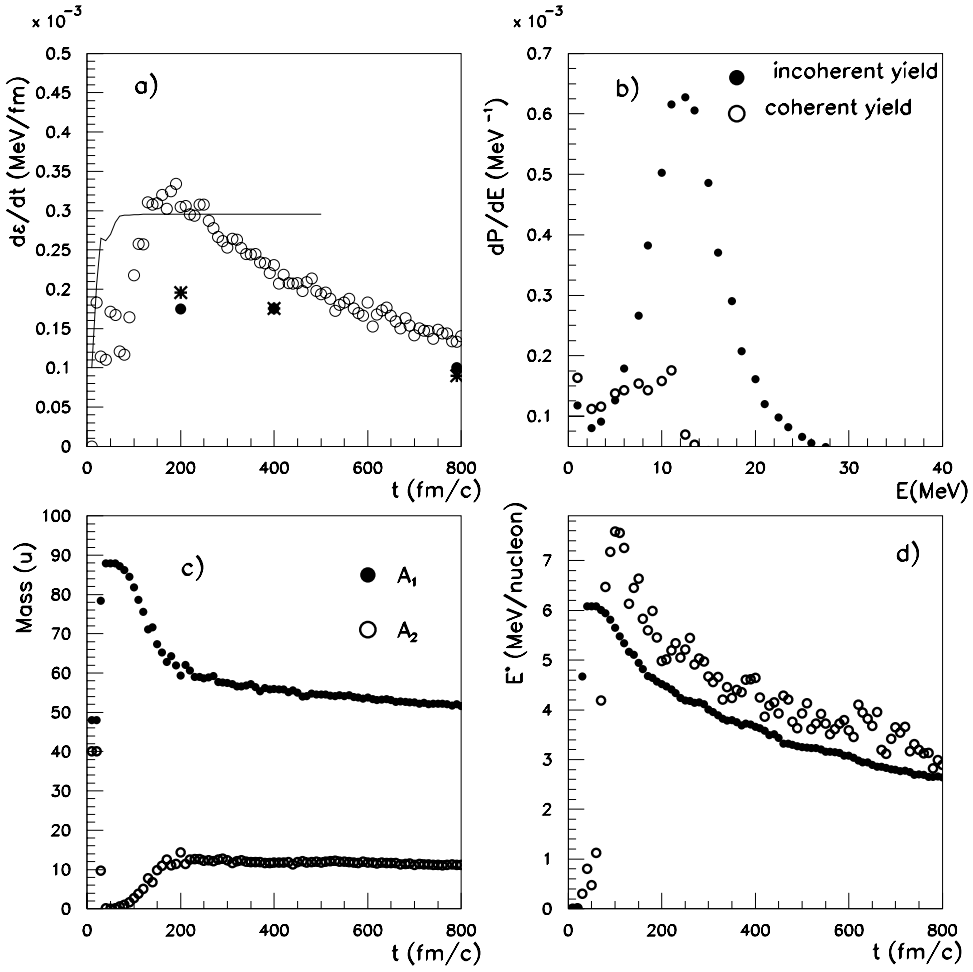

FIG. 8. For $E_{lab}=25$ MeV/nucleon and $b=0$ fm, (a) emitted power through the incoherent mechanism related to the Z component, as a function of time (empty circles) evaluated with CoMD calculations. In the same panel the stars represent the prediction of the CASCADE calculations for the collective emitted power at different times. The full circles represent the same quantity as predicted by CoMD calculations. The line represents the emitted power as a function of time produced by Langevin calculations applied to the total system. (b) Related γ-ray emission probability as a function of the energy for the incoherent (full circles) mechanism and for the coherent mechanisms (empty circles). (c) Average mass of the two largest fragments A_1, A_2 as a function of time. (d) Related average excitation energy per nucleon.

(with an average value corresponding to a density of about 70% of the saturation value) experienced by the system in the first 500 fm/c.

The width of the energy distribution shown in panel (b) is about 9 MeV. It is about 1.7 times the one shown in Fig. 5 for the ground state. It has to be noted, however, that the multiplicity distribution shown in Fig. 8(b) is the global result of a hot source which rapidly changes mass and excitation energy [see panels (c) and (d)]. In particular, in a short time the residues reach an excitation energy of about 4.5 MeV/nucleon and a mass of about 60 units. The changes in the following 600 fm/c are smaller.

Looking at the system behavior during a short time interval, clear preequilibrium effects can be seen from Fig. 8(a). In particular in the first 200 fm/c the power emitted via the incoherent mechanism increases up to a maximum value corresponding to the formation (on average) of the two main fragments. During this stage the collision rate increases practically with the same profile. The curve represents a prediction based on the Langevin approach [39] in which the damping parameter Γ and the resonant energy E_0 are computed from the γ-ray spectra obtained wiht our CoMD calculations. The mass A and the charge are those of the total system. The temperature has been computed from the usual relation for fermionic systems $E^*=aT^2$ with $a=A/12$ (the choice for the value of this parameter is discussed in the following section).

After a very short transient connected to the Γ parameter, we observe that the Langevin calculations [line in Fig. 8(a)] give a stationary value corresponding to the one predicted by statistical calculation [see Eq. (A9)].

This comparison shows that in this first stage the preequilibrium effect connected to the incoherent process is dominated by the finite time in which the collision rate (acting in this case as a noise able to excite the dipolar mode) increases. This time is larger than what the Langevin approach predicts. We note also that in the first 50–70 fm/c the emitted power evaluated with our calculations displays sharp

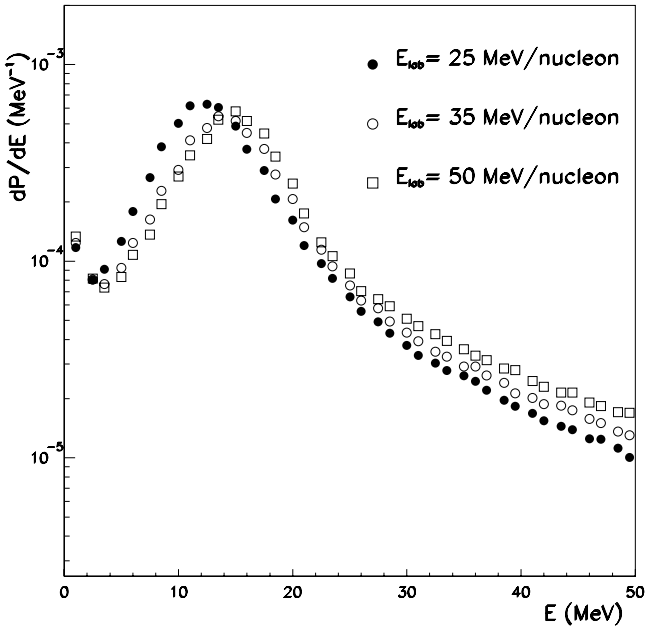

FIG. 9. Calculated γ-ray spectra at $b=0$ fm for the incoherent contribution and for three bombarding energies as indicated in the figure.

peaks which cannot be produced with the Langevin approach. These peaks originate from Coulomb and compression effects arising when the two nuclei start to overlap. Moreover, on average, a fragment starts to separate quickly from the total system [see Fig. 8(c)], and after 200 fm/c it is completely formed.

B. Comparison with the Langevin approach

To make a detailed comparison with statistical model calculations concerning the GDR mode, we have to disentangle between collective and noncollective or bremsstrahlung motion related to the total dipole. The presence of this last contribution can be seen in Fig. 9, where the spectra of the incoherent contribution are displayed in a semilogarithmic scale at different incident energies. The long tails at γ energies higher than 30 MeV are due to the bremsstrahlung.

To make this comparison we used the following procedure: at different time intervals the spectrum of the emitted radiation has been evaluated through a Fourier analysis whose details are given in Appendix B. The obtained spectra have been fitted with a function $F(E)$ reflecting the standard statistical model formula behavior plus an essentially exponential term able to reproduce the long tail related to the noncollective contribution [40,41]. From this procedure we have obtained the so-called temperature T, the GDR centroid, and the damping width parameter. These parameters describe the statistical collective mode through the first term F_R of the function $F(E)$ [see Eq. (B3)]. This procedure has been applied at different times and the extracted values of the T parameter have been correlated, by means of the well-known relation $E^*=(A/g)T^2$, to the calculated excitation energy of the hot source obtained from the CoMD calculations [see Figs. 8(d) and 8(c)]. The emitted power related to $F_R(E)$ represents the collective energy-weighted yield due to the motion along the Z direction produced by the dynamical model. It is shown with full circles in Fig. 8(a) at different times. We note that in the statistical model the parameter α in the first term of Eq. (B3) assumes the value $4e^2NZ\Gamma/3m_0A\pi(\hbar c)^2$ determined by the mass, charge, and damping width of the emitting source [see Eq. (B5)]. Therefore, using the average value of the above expression as evaluated with CoMD calculations, instead of the α value as extracted through the fit procedure, we can also obtain an estimation of the predicted strength according to the statistical calculations in the local time equilibrium hypothesis. The results are shown in Fig. 8(a) as stars, for different times.

From the calculations described, it results that at $E_{lab}=25$ MeV/nucleon, and for times greater than 200 fm/c, the CoMD predictions are in agreement with the statistical model (in the local time equilibrium hypothesis). This agreement is strongly supported by the fact that the g parameter used in the above-mentioned fit procedure assumes the value 12 at different impact parameters and at different times, within 10%. The stability of this parameter and its value, which is quite reasonable, also means that the CoMD calculations (at a relatively low energy and for times longer than the fragment formation one) produce fluctuations on the collective mode (with respect to the ensemble average), which have a reasonable size. This in turn means a substantial agreement, in this asymptotic limit, with the fluctuation dissipation theorem which [39], for such g parameter value and excitation energies, contains quantum mechanical effects ($T<E_0$) (see Appendix A).

To highlight this aspect, in Figs. 10(a) and 10(b) we show the calculations for the same initial condition by running the program without the constraint and the Pauli blocking correction factor in the collision term. It is clear from comparisons with Figs. 8(a) and 8(b) that the emitted power in this essentially classical case is a factor 10–20 times larger. In particular, the effects of the collectivity are washed out due to the rather broad spectrum of the incoherent contribution, and the coherent contribution (empty circles) is negligible in every energy region of the spectrum.

C. Coherent and incoherent contributions

After discussing the incoherent contribution obtained through CoMD calculations, we can make a self-consistent comparison with the coherent contribution obtained through the ensemble average using the same model. As already observed in Sec. II, we performed the same calculations for ^{40}Ca+^{48}Ca and for ^{40}Ca+^{46}Ti systems at 25 MeV/nucleon. The two systems display the same behavior for the incoherent contribution within 5%. For the impact-parameter selected window, which has been determined by the condition on the heavy residues (see Sec. II), we show in Fig. 11 the ratio R between the total γ-ray spectra (coherent plus incoherent contributions) for the ^{40}Ca+^{48}Ca and for the ^{40}Ca +^{46}Ti systems.

In these calculations the contribution due to the incoherent mechanism for times greater than 800 fm/c has been extrapolated asymptotically with a linear time law. This lin-

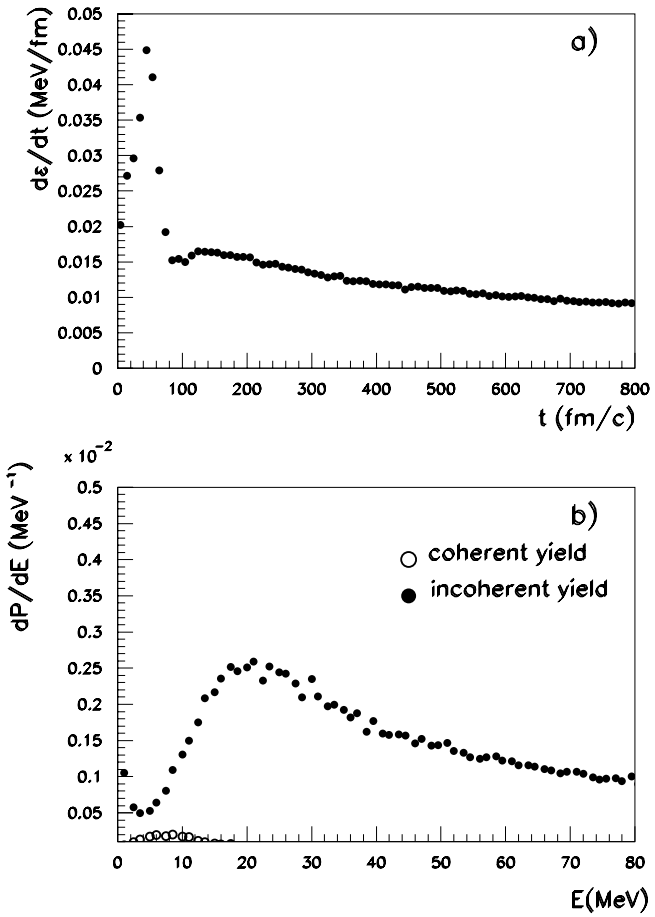

FIG. 10. For the ^{40}Ca+^{48}Ca system, (a) emitted power computed by means of the CoMD model without the constraint for $E_{lab}=25$ MeV/nucleon and $b=0$ fm, and (b) related γ-ray spectra for the coherent (empty circles) and incoherent (full circles) contributions.

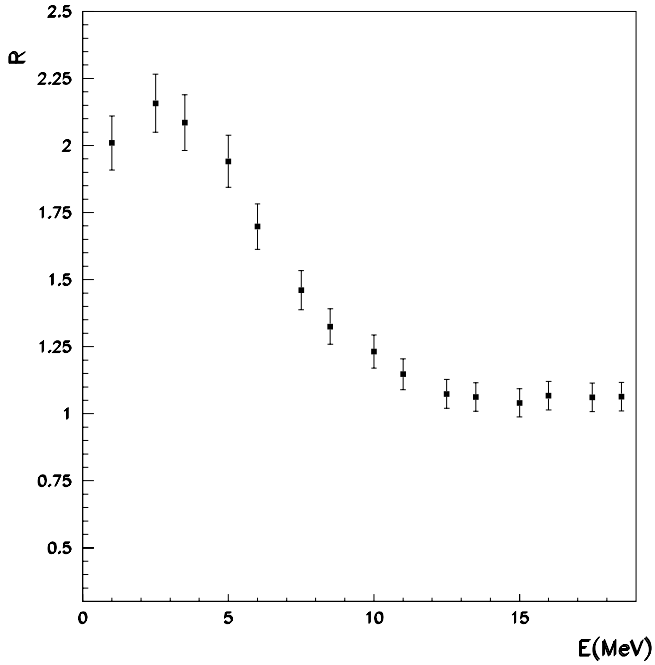

FIG. 11. Ratio R between the total γ-ray yield for the ^{40}Ca $+^{48}$Ca and ^{40}Ca+^{46}Ti as obtained by means of the model calculations for $E_{lab}=25$ MeV/nucleon. The involved impact parameters are distributed according to the b window selected by the coincidence with the heavy residues. The error bars indicate the global uncertainty related to the calculation (see Fig. 4 and the text).

earity is suggested by looking at the behavior of the incoherent emitted power evaluated for the two systems at times greater than 200 fm/c [see, for example, Fig. 8(a)]. This procedure can induce an error of the order of 20% on the estimate value of R.

The quantities plotted in Fig. 11 therefore represent the analog of the ratio between the experimental yields shown in the inset of Fig. 2. The analysis performed on the calculated quantities allows to state that at low energy, R values greater than 1 are due to the coherent contribution produced in the system ^{40}Ca+^{48}Ca. As already observed, this contribution in the ^{40}Ca+^{46}Ti system is about 20 times lower.

In particular by looking at Fig. 11 we note that the maximum in the ratio is located at energies lower than 5 MeV, whereas the maximum of the coherent contribution is peaked in the region around 10 MeV (see Fig. 8). This discrepancy is an effect related to the coherent and incoherent contribution tails. Experimentally (see the inset in Fig. 2) the ratio is peaked at higher energy because in reality the energy region lower than 5 MeV is dominated by the contributions coming from the low energy quadrupolar transitions and from the statistical dipolar emission produced in the last stages of the cascade. These two contributions have similar intensity (within 10%) for the investigated systems but are not described in the present study. For a more quantitative comparison we will consider the value of the ratios at 11 MeV. At this energy the experimental value of the ratio is about 1.3 (see Fig. 2), close to the maximum value, and the abovementioned contribution of the last stages of the cascade is small. Because of the small underestimation on the resonant energies (about 15%, see Sec. II A), this corresponds for our calculations to an energy of about 9 MeV. At this energy the estimated ratio is about 1.3 which is in good agreement with the experimental value for central collisions.

To summarize the results obtained for the system under study, we show in Table I the yield related to coherent contribution and the calculated ratio R compared with the experimental values.

V. RESULTS AT HIGHER ENERGY

In the previous sections we described, by means of the CoMD model, the experimental data shown in Sec. II. The low energy extra yield obtained for ^{40}Ca+^{48}Ca system, as compared with ^{40}Ca+^{46}Ti one, has been described as the effect of the large difference in the charge/mass ratio between ^{40}Ca and ^{48}Ca. This difference is in fact able to produce a coherent preequilibrium effect on γ-ray emission. Using our fully dynamical approach it has been shown that also the incoherent collective contribution can show preequilibrium effects mainly arising from the gradual opening of the phase space available for the nucleon-nucleon collisions. On the other hand, for the heavy residues formed after this short

TABLE I. Theoretical and experimental quantities for the investigated systems at 25 MeV/nucleon concerning the γ-ray yields and the corresponding ratios for the two systems. The quantities are related to the selected incomplete fusion events. dP^c/dE represents the theoretical predictions on the of γ-ray emission probability computed at $E_\gamma = 9$ MeV for the coherent process. dP^c_{exp}/dE represents the related experimental quantity evaluated at 11 MeV [11].

Mechanisms	$\frac{dP^c}{dE}$ (MeV^{-1})	$\frac{dP^c_{exp}}{dE}$ (MeV^{-1})	$R_{E_\gamma \simeq 9\ \mathrm{MeV}}$	$R^{exp}_{E_\gamma \simeq 11\ \mathrm{MeV}}$
Incomplete Fusion	2×10^{-4}	$(3\pm0.4)\times10^{-4}$	1.3 ± 0.1	1.3 ± 0.1

stage (about 200 fm/c), the results of the dynamical calculations seem to confirm that the collective γ-ray emission from the hot sources can be treated in the local time equilibrium hypothesis. In this section we want to extend the study of the nonequilibrium effects on the dipolar γ-ray emission to higher energy when the multifragmentation processes become prominent.

A. Coherent and incoherent processes versus incident energy for central collision

For central collisions ($b=0$ fm) we have performed calculations also at higher energy. In Figs. 12 and 13 for 35 and 50 MeV/nucleon, respectively, we plot the same quantities as shown in Fig. 8. At these energies the hot sources disassemble producing, on average, a third cluster [see Fig. 12(c)–13(c)]. The size of the largest fragment decreases by increasing the energy. The fragment formation process takes a shorter time, about 150 fm/c and 100 fm/c. As displayed in [see Fig. 12(d)–13(d)], the largest fragment reaches an average excitation energy of 5 MeV/nucleon within 200 fm/c.

In panel (a) of the same figures we show the emitted γ-ray power as a function of time produced by the incoherent mechanism. In panel (b) the γ-ray average multiplicity related to the coherent (empty circles) and incoherent (full

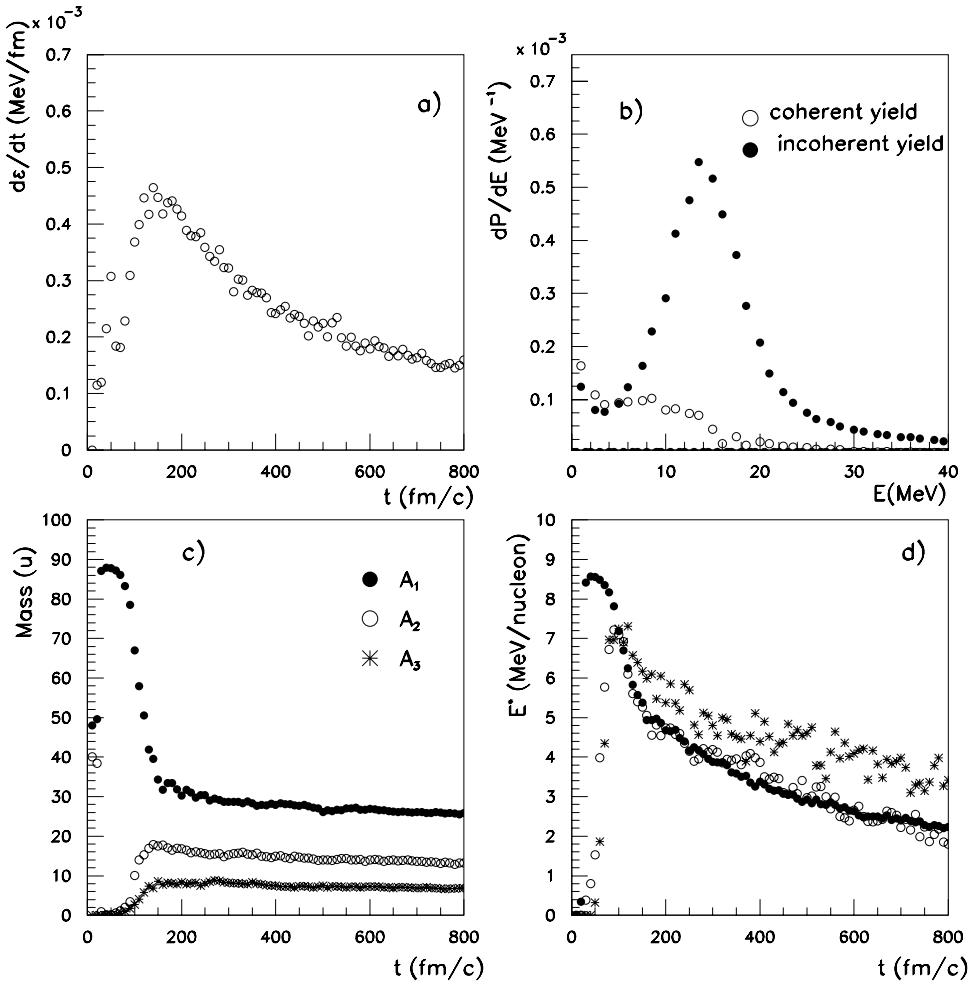

FIG. 12. Same as Fig. 8 but for $E_{lab}=35$ MeV/nucleon.

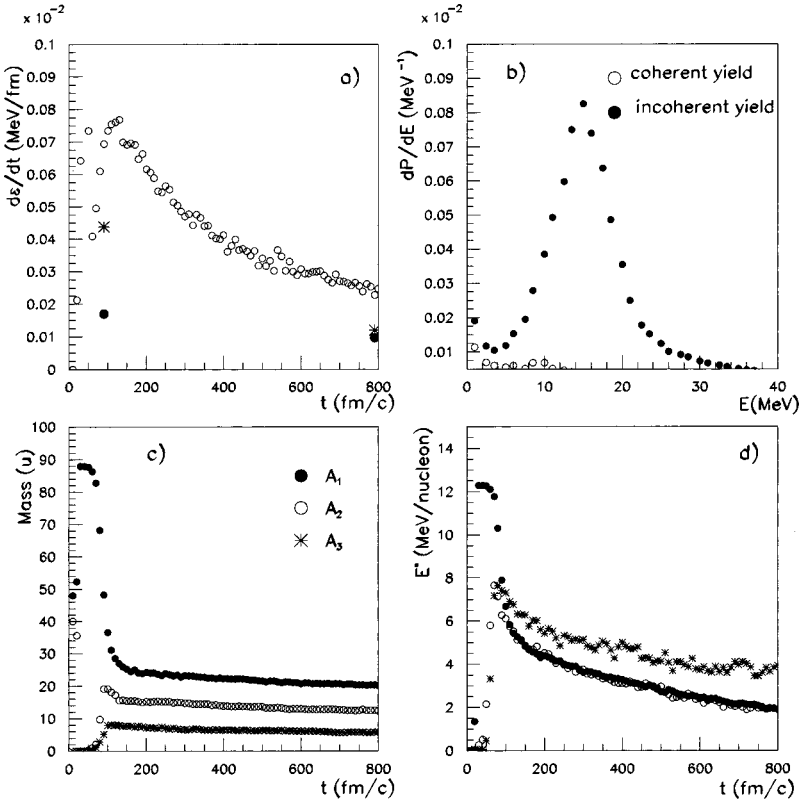

FIG. 13. Same as Fig. 8 but for E_{lab} = 50 MeV/nucleon.

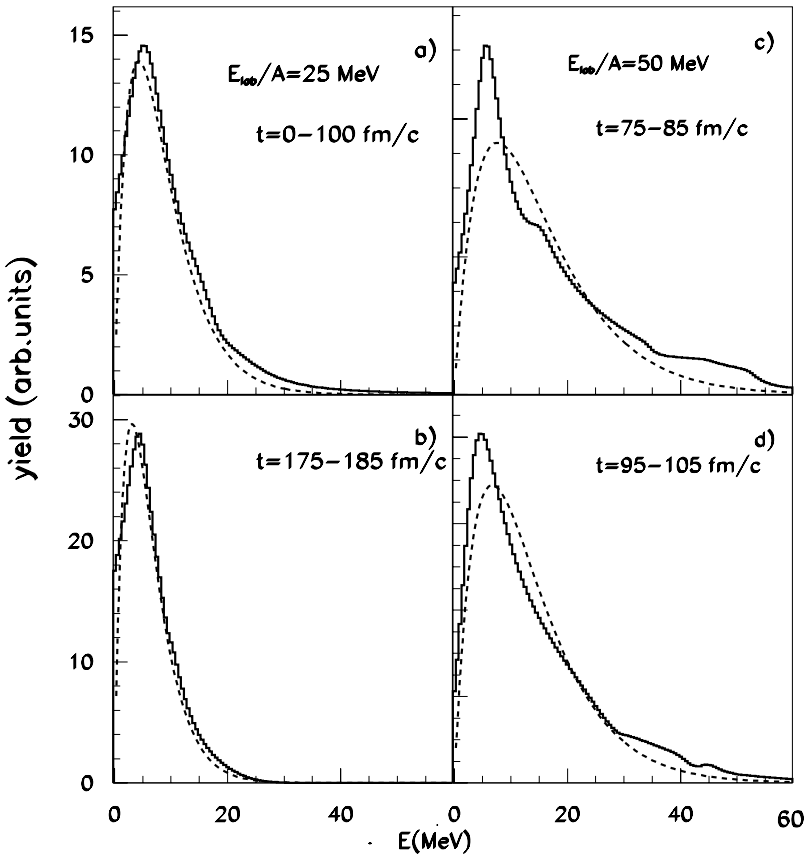

FIG. 14. In the different panels, the neutron energy spectra as obtained through the CoMD calculations are shown at different incident energies and at different emission times (full lines). The dot-dashed lines represent the fit with Maxwellian curves.

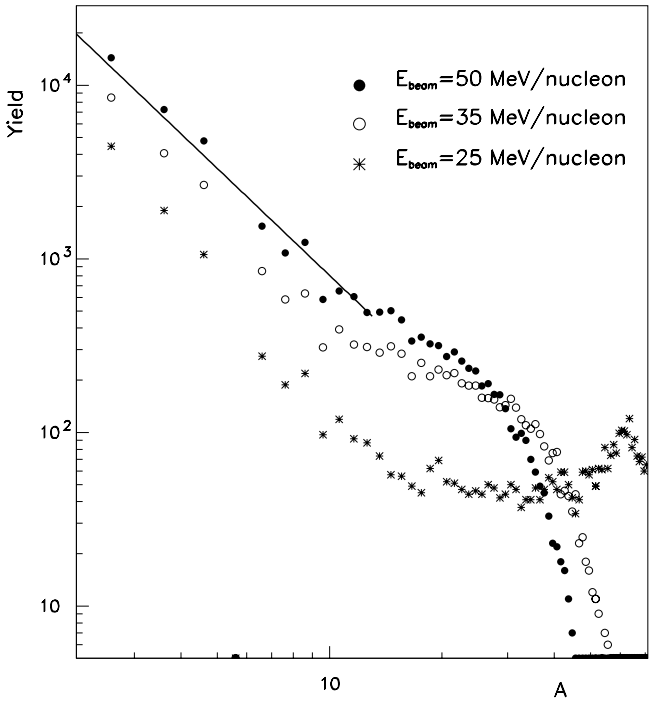

FIG. 15. Calculated mass spectra of the ^{40}Ca+^{48}Ca system for $b=0$ fm and at different energies. The line represents the results of the best fit with a power law for $E_{lab}=50$ MeV/nucleon.

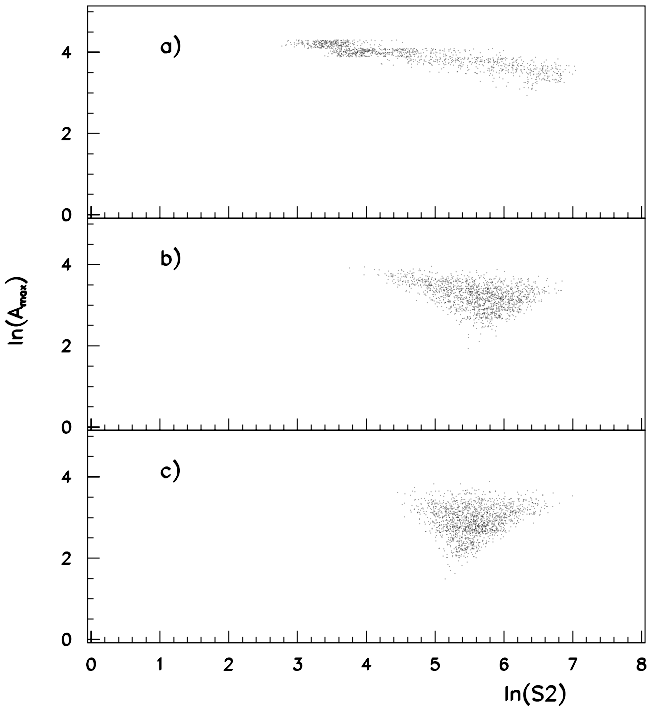

FIG. 16. Campi plot for central collisions in the system ^{40}Ca +^{48}Ca at different energies, (a) $E_{lab}=25$ MeV/nucleon, (b) $E_{lab}=35$ MeV/nucleon, and (c) $E_{lab}=50$ MeV/nucleon.

circles) emission is also shown.

The full circles in panel (a) of Fig. 13 represent the average incoherent collective strength, whereas the stars represent the statistical model prediction of the same quantity. The same criteria as for the 25 MeV/nucleon case have been used to estimate the collective yields, as given by the dynamical model, and the ones expected from the statistical model.

In contrast to the lower energy case, we note that around the time of the fragment formation, the predictions of the statistical model calculations overestimate the incoherent collective power emitted as predicted by our dynamical model. This effect is more evident at 50 MeV/nucleon. This suggests that by increasing the energy given to the system, the fluctuations in the collective mode are no longer in agreement with the predictions given by the Langevin approach or the standard statistical theory (see Appendix A). These deviations are more pronounced in the first stage of the interaction and they can show up after the fast fragment formation process when CASCADE calculations are usually applied.

To check if these nonequilibrium effects can be visible also for other degrees of freedom, in Fig. 14 we show the center of mass energy spectra of neutrons for central collisions at E_{lab} 25 MeV/nucleon and 50 MeV/nucleon. In panels (a) and (b), for the lower energy case, we show with full lines the spectra of neutrons emitted at different time intervals before and during the formation of fragments. In panels (c) and (d) the spectra for the 50 MeV/nucleon case are displayed. The dashed lines represent the results of a fit of the energy spectra with typical Maxwellian curves. The comparison with these curves shows that, apart from the deviation in the energy region of standard preequilibrium contribution (around 6 MeV and 12 MeV for beam incident energy equal to 25 MeV/nucleon and 50 MeV/nucleon, respectively), the strongest global deviation with respect to the Maxwellian shape is observed for the 50 MeV/nucleon case. We stress that this simple comparison with the Maxwellian curve is merely done to highlight qualitative differences between particle spectra. It is moreover possible to show (by comparing the neutron spectra with those obtained when the neutrons are on the surface of the hot sources) that these differences are due to strong mean field instabilities present at the surface of the hot sources produced at 35 and 50 MeV/nucleon up to about 300 fm/c for this last case.

These instability effects can be investigated, as it is usually done, by looking at many-body quantities such as the fragments, and their energy and mass distributions (see as an example Ref. [42]). In Figs. 15 and 16 we show the mass distributions and the relative Campi plots at 35 MeV/nucleon and 50 MeV/nucleon. From these figures the typical conditions for a phase transition with a power law for the mass distributions (shown by a straight line) and bending of the Campi plot are clearly evident.

For a system undergoing a multifragmentation process, this analysis therefore seems to suggest a growth of fluctuations on the dipolar mode and a decreasing collective contribution with respect to the standard statistical approach.

This means that, at a macroscopic level, the equation of motion of the dipole deviates from the simple prescription of a Langevin approach described in Appendix A. This deviation does not seem to be due to the well-known effects such as those that can be taken into account using a local time equilibrium hypothesis as previously discussed. On the contrary, this deviation seems to arise from a more complex

TABLE II. Degree of collectivity and degree of coherence, as defined in Secs. V B and V C, estimated through CoMD calculations for central collision at different incident energies and at different times.

E_{lab} (MeV/nucleon)	$\varphi_c(tf,tm)$	$\varphi_c(0,tf)$	$\varphi_{ch}(0,tm)$	$\varphi'_c(tf,tm)$	$\varphi'_c(0,tf)$	$\varphi'_{ch}(0,tm)$
25	0.89	0.78	0.095	1	1	1
35	0.86	0.62	0.064	0.96	0.80	0.67
50	0.83	0.58	0.059	0.93	0.74	0.62

form of the effective Hamiltonian describing the collective mode during a multifragmentation process, or it can be simply related to the inapplicability of the temperature concept for the collective motion.

B. Degree of dipolar collectivity in central collision as function of energy

To make the performed study more quantitative, in this section we want to estimate a degree of collectivity for the incoherent motion in central collisions.

For this purpose, starting from the results already shown in Figs. 8, 12, and 13 and using relations (B1)–(B4), we computed the following quantities:

$$W^{<}_{Es}(t)=\int_0^{Es} W^{<}(E,t)dE, \tag{5}$$

$$W^{>}_{Es}(t)=\int_0^{Es} W^{>}(E,t)dE, \tag{6}$$

$$\varepsilon_{Es}(0,t)=W^{<}_{Es}(tm)-W^{>}_{Es}(t), \tag{7}$$

$$\varepsilon_{Es}(t,tm)=W^{>}_{Es}(t). \tag{8}$$

In these equations Es represents an upper limit for the energy integration, which we have fixed at 35 MeV. Moreover, using a fit procedure similar to the one used in the preceding section, we have separated the collective contribution $\varepsilon_{Es,c}$ from the bremsstrahlung one. In such a way we have defined the degree of collectivity at different time intervals as

$$\varphi_c(0,t)\equiv\frac{\varepsilon_{Es,c}(0,t)}{\varepsilon_{Es}(0,t)}, \tag{9}$$

$$\varphi_c(t,tm)\equiv\frac{\varepsilon_{Es,c}(t,tm)}{\varepsilon_{Es}(t,tm)}, \tag{10}$$

where t has been chosen as the time of fragmentation of the hot sources, t_f. Its values are about 180 fm/c, 135 fm/c, and 90 fm/c at 25 MeV/nucleon, 35 MeV/nucleon, and 50 MeV/nucleon, respectively. The results of these calculations are shown in Table II. By comparing the results of the second and third column, it becomes evident that the degree of collectivity is not uniformly distributed in time. In particular, $\varphi_c(tf,tm)$ slowly decreases with the increase in energy.

Fast changes and a much lower value of the collectivity are instead observed during and before the fragment formation, as one can see from the behavior of $\varphi_c(0,tf)$. This time region is the same where the strongest deviations from the standard statistical model have been discussed in the preceding section. It is worthwhile noting that remarkable changes are between 25 and 35 MeV/nucleon when the multifragmentation process sets in. This suggests a strong correlation of the phenomenon with the disassembly of the system and with the increasing of the bremsstrahlung contribution. From our calculations, using the described fit procedure on the γ-ray probability emission [see Eq. (B5)], the NZ/A value necessary to get the agreement with the statistical model calculations is lower than the calculated value obtained through the dynamical approach by looking at the charge and mass of the hot source. This clearly gives strong support to the existence of preequilibrium effects of the incoherent or statistical emission mechanism produced by the separation of different phases in the system. A possible explanation is that during the fragment formation process only a reduced number of nucleons are able to follow a collective mode because of the redistribution of the nucleons into different fragments.

We conclude this section by observing that the large changes of the degree of collectivity, being concentrated in short time, involve only a small fraction of the total yield. This obviously can make, in some cases, the experimental investigation rather ambiguous. In the following section we will discuss this problem by analyzing the degree of coherence of the dipolar mode.

C. Degree of coherence

In this section we show the results concerning the coherent contribution at the different energies for central collisions ($b=0$ fm). In Fig. 17 we show the ratio R between the total yield (coherent and incoherent) and the incoherent one as a function of γ energy at different incident energies. The ratios show a bump peaked at around 3 MeV. The higher values are obtained at 25 MeV/nucleon, for which the peak reaches the value 1.6. The visibility of the extra yield and the related energy distribution become weaker and wider by increasing the incident energy. This is due to the increased collision rate and to the fragment formation process being able to destroy the phase relation between the collective oscillations belonging to the same ensemble of events.

We can define a degree of coherence, $\varphi_{ch}(0,tm)$, for the collective motion by performing the ratio between the total energy emitted via the coherent mechanism and the one emitted by the incoherent one according to the following relation:

$$\varphi_{ch}(0,tm)\equiv\frac{\varepsilon_{Es,ch}(0,tm)}{\varepsilon_{Es}(0,tm)}, \tag{11}$$

where the quantity $\varepsilon_{Es,ch}(0,tm)$ is the analog of $\varepsilon_{Es,c}(0,tm)$

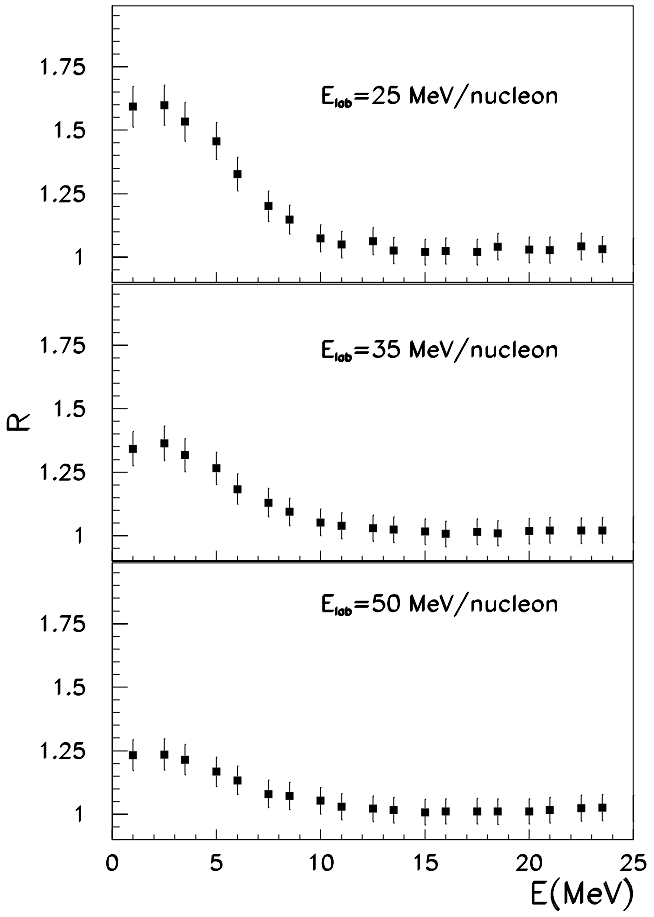

FIG. 17. Ratio R between the total γ-ray yield for the ^{40}Ca $+^{48}$Ca and ^{40}Ca$+^{46}$Ti as obtained by means of the model calculations at $b=0$ fm and at different energies. The error bars indicate the global uncertainty related to the calculations.

defined in Eqs. (7) and (8), but it is relative to the emitted power connected to the coherent process. Es has been set equal to 20 MeV and tm to 1000 fm/c.

The results are shown in Table II in the fourth column. It is remarkable that the behavior of the degree of coherence resembles the behavior of the degree of collectivity for the incoherent process $\varphi_c(0,t_f)$, which has been defined in a time interval around the fragment formation process. In particular, large changes are observed between 25 and 35 MeV/nucleon when the instability leading to the fragment formation sets in.

This similar behavior is better seen by looking at the columns 5–7 of Table II in which the degree of collectivity and the degree of coherence have been normalized to the 25 MeV/nucleon case. They have been indicated with the corresponding primed symbols.

From this analysis it seems that the degree of collectivity of the incoherent contribution in the first one is $\simeq$200 fm/c and the degree of coherence of the mode are linked. Moreover, the relative changes of the degree of coherence also appear to be more sensitive to the variation of the bombarding energy and to the related main reaction mechanism.

We conclude this section by observing that, from an experimental point of view, the study of the coherent contribution has been performed in the last experiments, such as that discussed in this work, through a direct comparison between very similar systems having only large differences in the charge/mass symmetry of the two partners. The visibility of the coherent contribution has been already discussed. In particular, it has been shown in Sec. III that the different charge/mass of the colliding nuclei can be used as a marker of the dynamics in the first hundreds of fm/c. In this case a related coherence length in time $t_{ch}\simeq\hbar/\Gamma_{ch}$ could be also estimated from the damping width Γ_{ch} of the coherent contribution. The results shown in this section further strongly suggest that the study of the coherent contribution can give useful information about the the degree of collectivity of nuclear matter as a function of energy. This information moreover can show a higher degree of sensitivity with respect to the one obtained by looking, as usually done, only to the GDR statistical emission.

D. Concluding remarks

In this work the properties of the coherent and incoherent γ-ray emission have been studied for the ^{40}Ca$+^{48}$Ca and ^{46}Ti systems at different incident energies and for essentially incomplete-fusion reaction mechanisms. This study has been performed using the recently developed CoMD model.

The coherent contribution to the γ-ray emission obtained through the ensemble average of the time evolution of the total dipole is able to justify, in a quantitative way, the extra yield observed in the experimental data collected for the system under study. Moreover, because of the short time scale during which this coherent process evolves, its main behavior is heavily affected by the other fast changing properties of the hot compound as, for example, the degree of deformation and expansion, and the average nucleon-nucleon collision rate. The comparison between the dynamical calculations obtained from the present model concerning the incoherent contribution, and the standard statistical model show a substantial agreement at long times (800–1000 fm/c). This agreement is referred to the late stage of the interaction when any dynamical effect is ceased and the system is thermalized. Therefore in the CoMD, because of the constraint, the fluctuations on the collective dipolar mode are in good agreement with those produced from CASCADE calculations using a density level parameter $a\simeq A/12$.

The agreement observed in this kind of asymptotic limit allows us to investigate with more confidence the properties of the fluctuating dipolar collective mode also in short time interval. In particular, at 25 MeV/nucleon a comparison between the experimental values and the calculated ratios for the total and the incoherent yield has been performed at different impact parameters for the selected window through the experimental constraint. The correlations between the reaction mechanisms and the intensity of the γ-ray extra yield have been reproduced by the model calculations. These correlations concern not only the average fragment mass produced in the reactions but also the shape of fragment kinetic energy spectra.

For central collisions, the more detailed study of the incoherent collective yield at different times has instead shown deviations with respect the standard statistical model and the Langevin approach at times before and around the time of the fragment formation process. These kind of effects, which can be also regarded like preequilibrium effects, become prominent at 35 and 50 MeV/nucleon when the hot sources experience a multifragmentation process.

In particular, under these conditions the degree of collectivity, as predicted by the CoMD model, is lower than the value predicted according to the compound nucleus hypothesis. This lowering also persists using the local time equilibrium hypothesis typical of the hybrid models. The analysis performed on the spectral properties of the emitted power suggests that part of the system is no more able to follow the collective vibration during the first moment of the interaction, and during the fragment formation process. However, this kind of phenomenon is rather short in time, and it involves about 15–20% of the total emitted power in the first 1000 fm/c.

The degree of collectivity has been evaluated at different incident energies and it shows the largest changes (in the first 180 fm/c) between 25 and 35 MeV/nucleon just when a transition from a predominant binary to multifragmentation process is seen. Finally, the degree of coherence of the proton vs neutron motion has been also estimated and its relative change with the incident energy shows strong correlations with the degree of collectivity of the incoherent motion, revealing also a higher sensitivity to the changes of excitation energy.

Therefore we believe that the existence of such a correlation could be used with advantage from an experimental point of view. In fact, the coherent process can be, in principle, directly revealed (like in Refs. [11,18]) by comparing very similar systems with different charge/mass asymmetry distribution between the colliding nuclei. Studies of the evolution of the coherent yield as a function of the incident energy could therefore give useful information for the research lines which aim to investigate the correlations between the existence of the standard GDR mode and the phase transitions in very hot systems [5,6,11]

Finally, the extra yield of the coherent contribution with respect to the incoherent one seems to show the largest contribution at energies where other mechanisms of emission, occurring in the last stage of the cascade, are dominant. Therefore measurements where multiple quadrupolar low energy γ-ray cascades can be discriminated could be useful to investigate experimentally the extra yield also in low energy region.

ACKNOWLEDGMENTS

We thank F. Ferrera for his help during the compilation phase of our program. We also thank Dr. J. S. Winfield for his kind help in the revision of the text.

APPENDIX A

For the total dipole expressed in units of elementary charge we can write the one dimensional Langevin equation as

$$\frac{d^2D^i}{d^2t} = -(\omega_0)^2 D^i - \gamma \frac{dD^i}{dt} + \chi^i(t). \tag{A1}$$

The time t is expressed in fm/c. $\chi^i(t)$ represents the stochastic force [$\overline{\chi^i(t)} = 0$] acting for each event i. The damping Γ of the collective mode is related to the friction coefficient through the following relation $\Gamma = \gamma \hbar c$.

The solution of this equation can be expressed as the sum of two terms:

$$D^i(t) = \overline{D(t)} + D^i_f(t). \tag{A2}$$

The last term in the right hand side of the above equation represents the so-called incoherent or fluctuating contribution since $\overline{D^i_f(t)} = 0$, whereas the first term represents the ensemble average or the coherent part of our quantity. The ensemble average can be easily integrated:

$$\overline{D(t)} = e^{-\gamma t}\left[D(0)\cos(qt) + \frac{V(0) + \gamma X_0}{q}\sin(qt) \right], \tag{A3}$$

whereas for the fluctuating part we consider the following general solution:

$$D^i_f(t) = \frac{1}{q}\int_0^t e^{-(\gamma/2)(t-t')}\sin[q(t-t')\chi^i(t')]dt', \tag{A4}$$

with

$$q = \sqrt{\omega_0^2 - \left(\frac{\gamma}{2}\right)^2},$$

where $V(t) = dD(t)/dt$.

In Eq. (A2) the first term is completely determined by fixing the initial conditions $\overline{D(t)} \equiv D(0)$ and $\overline{V(t)} \equiv V(0)$.

For example, in a heavy ion collision, if we choose as time reference the time when the two nuclei start to touch, and we neglect polarization effects due to the Coulomb interaction, $D(0)$ can be expressed as [14]

$$D(0) = \frac{1}{2}\frac{A_p A_t}{A_p + A_t}\left(\frac{N_t - Z_t}{A_t} - \frac{N_p - Z_p}{A_p}\right)R \equiv \frac{1}{2}\mu Y R, \tag{A5}$$

where R is the contact distance. It is always different from zero if the two partners have a different charge/mass ratio. The time derivative of the previous expression at the contact point fixes the initial condition related to $V(0)$, which can be expressed through the sum of several terms. One of these terms is proportional to dR/dt, therefore it increases with the bombarding energy (it gives a small contribution to the non-equilibrium condition for $E_{lab} < 10$ MeV/nucleon). The other terms arise from the time derivative of the reduced mass and of the charge/mass asymmetry differences Y between the partners of the binary system. These variables can assume a very small value at the time of contact if the flux of mass and charge at this time has a maximum.

We note that because of the structure of Eqs. (A1) and (A2), the average total power emitted has the following semiclassical expression evaluated through the Larmor formula:

$$\frac{d\epsilon}{dt}=\frac{2}{3}e^2\overline{\frac{d^2D^i(t)}{dt}^2}=\frac{2}{3}e^2\left[\left(\frac{d\bar{V}}{dt}\right)^2+\left(\overline{\frac{dV_f^i}{dt}}\right)^2\right]. \quad \text{(A6)}$$

The first term represents the so-called coherent contribution to the γ-ray yield and the second the incoherent or fluctuating one.

To evaluate the fluctuating contribution, it is necessary to specify the time correlation properties of the stochastic force [see Eq. (A7)]. Using the fluctuation dissipation theorem [39], we get

$$C(t-t')=\overline{\chi^i(t)\chi^i(t')}=\frac{4\Gamma A}{2\pi(\hbar c)^2 m_0}\frac{A}{NZ}\frac{\cos(\theta_T)}{\frac{(t-t')^2}{(\hbar c)^2}+\frac{1}{T^2}}, \quad \text{(A7)}$$

$$\theta_T=2\left[\arctan\left(\frac{(t-t')T}{\hbar c}\right)\right],$$

where T is the temperature, m_0 is the nucleon mass, and NZ/A is the reduced mass number of the neutron and proton relative motion. In the above expression the zero-point motion has been subtracted.

The framework offered by this approach is rather simple; the collective coordinate is explicitly introduced, the system under study is closed (or infinite). This means that the mass related to the collective motion is constant. Moreover, the fluctuation dissipation theorem implies that the response and correlation function are calculated with a canonical microscopic distribution characterized by a fixed value of the temperature T. The total energy of the thermal bath is constant, and therefore the energy of the collective mode is supposed to be negligible with respect to the thermal one. Moreover, it is worthwhile noting that, even if rather simple, this model contains quantum mechanical effects for $T<\hbar\omega_0$, because the correlation function related to the stochastic force has a finite length in time.

Now starting from the general solution [Eq. (A4)] and using Eq. (A7), it is possible to compute the following ensemble averages:

$$\overline{\frac{d^2D_f^i}{dt^2}}^2=\omega_0^4\overline{(D_f^i)^2}+\frac{\Gamma}{\hbar c}^2\overline{(V_f^i)^2}+2\omega_0^2\frac{\Gamma}{\hbar c}\overline{V_f^iD_f^i}-2\omega_0^2\overline{D_f^i\chi_i}-2\frac{\Gamma}{\hbar c}\overline{V_f^i\chi_i}+\overline{\chi_i^2}. \quad \text{(A8)}$$

In particular,

$$\overline{(D_f^i)^2}=\frac{1}{q^2}I^2(s,s),$$

$$\overline{V_f^{2,i}}=\frac{\Gamma^2}{(4\hbar cq)^2}I^2(s,s)+I^2(c,c)-\frac{\Gamma}{(\hbar cq)}I^2(s,c),$$

$$\overline{V_f^iD_f^i}=-\frac{\Gamma}{2\hbar cq^2}I^2(s,s)+\frac{1}{q}I^2(s,c),$$

$$\overline{D_f^i\chi_i}=\frac{1}{q}I(c),$$

$$\overline{V_f^i\chi_i}=I(c)-\frac{\Gamma}{2\hbar cq}I(s),$$

$$\overline{\chi_i^2}=\frac{2m_0\Gamma AT}{\hbar cNZ},$$

with

$$I^2(s[c],s[c],t)=\int_0^t\int_0^t e^{-\gamma/\hbar c(t-t')}e^{-\gamma/\hbar c(t-t'')}\times\sin[\cos][q(t-t')]\sin[\cos]\times[q(t-t'')]C(t'-t'')dt'dt'',$$

$$I(s[c],t)=\int_0^t e^{-\gamma/\hbar c(t-t')}\sin[\cos][q(t-t')]C(t')dt'.$$

The evaluation of the above expressions shows that while the average dipole follows a damped oscillating behavior, the root mean square of the fluctuating part increases in the same time interval $t\simeq\hbar/\Gamma$ up to a stationary and constant value.

In the uncorrelated three-dimensional and isotropic case, it is easy to show (see Ref. [39], pp. 415, 428) that the stationary value of the emitted power for each component is described by the following relation:

$$\left(\frac{d\epsilon}{dt}\right)^{t\gg\hbar/\Gamma}=\frac{4e^2NZ\Gamma}{9m_0A\pi(\hbar c)^2}\int_0^\infty\frac{e^{-E/T}}{(E^2-E_0^2)^2+(E\Gamma)^2}E^5dE=\int_0^\infty E\frac{d^2P}{dEdt}dE, \quad \text{(A9)}$$

where E is the γ energy and $E_0=\hbar\omega_0$.

The quantity $d^2P/dEdt$ represents the number of γ emitted in the time and energy units. It agrees with standard statistical theory of the compound nucleus system and represents the heart of the statistical CASCADE code calculations [31]. The calculations based on this simple approach are used as an useful comparisons with CoMD calculation in Sec IV B.

APPENDIX B

To make a comparison with statistical model calculations or Langevin calculations [see Eq. (A9)] we need to evaluate the spectral properties of the emitted power at different times as obtained from CoMD calculations. For the systems studied, we performed the above comparison by numerically

evaluating expressions (B1) and (B2). Each ensemble of events is characterized by a fixed value of the impact parameter and incident energy,

$$\left(\frac{d^2P}{dEdt}\right)_t \simeq \frac{W^<(E,t-\Delta t/2)-W^<(E,t+\Delta t/2)}{E\Delta t} \quad \text{(B1)}$$

for $t \geqslant 500$ fm/c, and

$$\left(\frac{d^2P}{dEdt}\right)_t \simeq \frac{W^>(E,t+\Delta t/2)-W^>(E,t-\Delta t/2)}{E\Delta t} \quad \text{(B2)}$$

for $t<500$ fm/c.

Δt is about 150 fm/c in both cases. The quantities appearing in the numerators are defined in this way:

$$W^<(E,t)=\frac{2}{3\pi\hbar c}\overline{\left|\int_0^{t+\Delta t/2}\frac{dV^i_{Z,f}}{dt}e^{-iEt/\hbar c}dt\right|^2},$$

$$W^>(E,t)=\frac{2}{3\pi\hbar c}\overline{\left|\int_{t-\Delta t/2}^{t_m}\frac{dV^i_{Z,f}}{dt}e^{-iEt/\hbar c}dt\right|^2}, \quad \text{(B3)}$$

where $t_m=1000$ fm/c is the time interval during which the dynamical evolution has been followed. Obviously, all the expressions have been evaluated for discrete values of energy $n\pi\hbar c/t_m$ and time $n\delta t$. δt is the time step for the integration of the equation of motion in the CoMD calculations. Therefore the integrals have been substituted by discrete sums according to the expression for the discrete Fourier transform. The above relations give us an estimation of the spectral properties of the emitted power at each time related to the Z dipolar component. The corresponding spectra $(d^2P/dEdt)_t$ have been fitted with a function $F(E)$ able to reproduce the statistical model formula plus terms able to reproduce the long tail due to the noncollective contribution, i.e.,

$$F(E)=F_R(E)+F_{NR}(E),$$

$$F_R(E)=\alpha\frac{e^{-E/T}}{(E^2-E_0^2)^2+(E\Gamma)^2}E^4,$$

$$F_{NR}(E)=\beta e^{-E/T'}+\frac{\psi}{E}. \quad \text{(B4)}$$

The fit procedure has been performed to reproduce the shape and the energy-weighted integrated yield up to a maximum $E_{max}=\pi\hbar/\delta t$.

From this procedure we obtained, apart from the coefficients α,β,ψ,T', the temperature T, the GDR centroid E_0, and the damping width Γ describing the statistical collective mode.

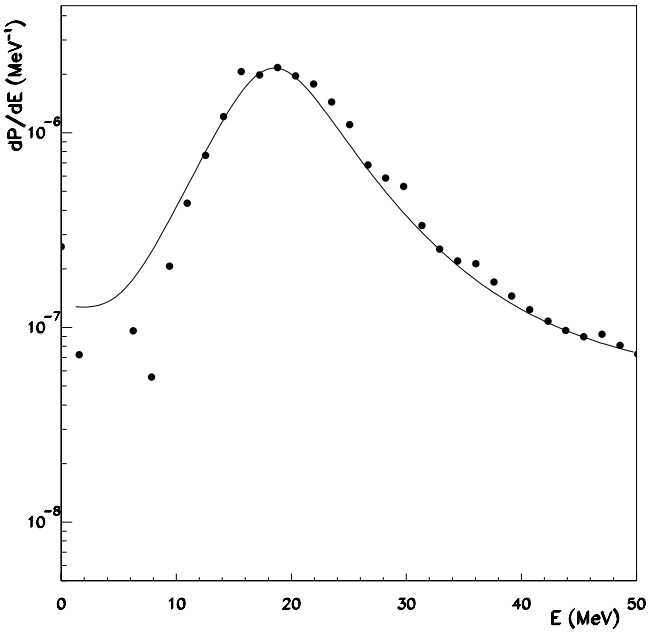

FIG. 18. γ-Ray spectrum for the radiation emitted around 800 fm/c for the ^{40}Ca+^{48}Ca system at $E_{lab}=25$ MeV/nucleon and $b=0$ fm. The curve represents the result of the fit procedure [see Appendix B and Eq. (B4)]. Some of the extracted parameters have the following values within the uncertainty of 10%: $\Gamma=12$ MeV, $E_0=18$ MeV, $g=12$, and $T=6.5$ MeV.

The energy-weighted integrated yield $\int_0^{E_{max}}EF_R dE$ (evaluated in the discrete approximation) can therefore represent the collective contribution due to the motion produced by the CoMD model (see Sec. IV B).

An example of the described fit procedure on the emitted power at $t\simeq 800$ fm/c for the ^{40}Ca+^{48}Ca system at 25 MeV/nucleon and $b=0$ fm is shown in Fig. 18. The curve corresponds to the following parameters for the collective mode: $\Gamma=12$ MeV, $E_0=19$ MeV, $g=12$, and $T=6.5$ MeV within 10% uncertainty. Finally, by comparing expressions (B3) and (B4) with Eq. (A9), it is possible to note that in the local time equilibrium hypothesis the following equality holds:

$$\alpha=\frac{4e^2NZ\Gamma}{3m_0A\pi(\hbar c)^2}. \quad \text{(B5)}$$

Here N, Z, and Γ represent the neutron number, proton number, and the GDR damping width of the emitting source, respectively.

[1] K.A. Snover, Annu. Rev. Nucl. Part. Sci. **36**, 545 (1986).
[2] J.J. Gaardhøje, Annu. Rev. Nucl. Part. Sci. **42**, 483 (1992).
[3] N.P. Shaw *et al.*, Phys. Rev. C **61**, 044612 (2000).
[4] S.K. Hui *et al.*, Phys. Rev. C **62**, 054604 (2000).
[5] J.J. Gaardhoje, A.M. Bruce, and B. Herskind, Nucl. Phys. **A482**, 121c (1988).
[6] T. Suomijarvi *et al.*, Phys. Rev. C **53**, 2258 (1996).
[7] A.L. Goodman and T. Jin, Phys. Rev. C **54**, 1165 (1996).

[8] M. Thoennessen, RIKEN Rev. **2**, 132 (1999).
[9] K.A. Snover, Nucl. Phys. **A687**, 337c (2001).
[10] P. Heckman *et al.*, Nucl. Phys. **A687**, 225c (2001).
[11] S. Tudisco *et al.*, Europhys. Lett. **58**, 811 (2001).
[12] F. Amorini, M. Cabibbo, G. Cardella, A. Di Pietro, P. Figuera, A. Musumarra, M. Papa, G. Pappalardo, F. Rizzo, and S. Tudisco, Phys. Rev. C **58**, 987 (1998).
[13] M. Papa *et al.*, in *Proceedings of the Eighth International Conference on Nuclear Reaction Mechanisms, Varenna, 1997* edited by E. Gadioli (Universita Degli Studi Di Milano, Milano, Italy, 1937).
[14] M. Papa *et al.*, Eur. Phys. J. A **4**, 69 (1999).
[15] S. Kamanin, A. Kugler, Yu.G. Sobolev, and A.S. Fommichev, Z. Phys. A **337**, 111 (1990); L. Campaiola *et al.*, Nucl. Phys. **A583**, 119 (1995).
[16] L. Campaiola *et al.*, Nucl. Phys. **A583**, 119 (1995).
[17] L. Campaiola *et al.*, Z. Phys. A **352**, 421 (1995).
[18] S. Flibotte *et al.*, Phys. Rev. Lett. **77**, 1448 (1996).
[19] D. Pierroutsakou *et al.*, Nucl. Phys. **A687**, 245c (2001).
[20] D.M. Brink, Nucl. Phys. **A519**, 3c (1990).
[21] Ph. Chomaz, M. Di Toro, and A. Smerzi, Nucl. Phys. **A563**, 509 (1993).
[22] C. Yanhuang, M. Di Toro, M. Papa, A. Smerzi, and Z. Jiquan, in *Proceedings of the International Conference on Dynamical Features of Nuclei and Finite Systems, Barcelone, 1993*, edited by X. Vinas (World Scientific, Singapore, 1994).
[23] P.F. Bortignon *et al.*, Nucl. Phys. **A588**, 101c (1995).
[24] V. Baran, D.M. Brink, M. Colonna, and M. Di Toro, Phys. Rev. Lett. **87**, 182501 (2001).
[25] A. Bonasera, F. Gulminelli, and J. Molitoris, Phys. Rep. **243**, 1 (1994).
[26] M. Papa, F. Amorini, A. Di Pietro, G. Cardella, P. Figuera, A. Musumarra, G. Pappalardo, F. Rizzo, and S. Tudisco in *Proceedings of the International Conference Nuclear Reaction and Beyond, Lanzhou, 1999* edited by G.M. Jin (World Scientific, Singapore, 2000).
[27] M. Papa, T. Maruyama, and A. Bonasera, Phys. Rev. C **64**, 024612 (2001).
[28] T. Maruyama, A. Bonasera, M. Papa, and A. Shiba, J. Nucl. Radiochem. Sci. **3**, 77 (2002).
[29] M. Papa, T. Maruyama, and A. Bonasera, in *Proceedings of the International Conference on Nuclear Physicsat Border Line, Lipari, 2001*, edited by G. Giardina (World Scientific, Singapore, 2002).
[30] M. Papa, G. Cardella, A. Bonasera, and T. Maruyama, Heavy Ion Phys. **16**, 223 (2002).
[31] F. Puhlhofer, Nucl. Phys. **A280**, 267 (1977).
[32] G. Pappalardo, Nucl. Phys. **A488**, 395c (1988).
[33] M. Papa *et al.*, Phys. Rev. C **61**, 044614 (2000).
[34] H. Nifenecker and J.A. Pinston, Annu. Rev. Nucl. Part. Sci. **40**, 113 (1990); P. Sapienza *et al.*, Nuovo Cimento **111**, 999 (1998).
[35] T.M.V. Bootsma *et al.*, Z. Phys. A **359**, 391 (1997).
[36] R.J. Charity *et al.*, Nucl. Phys. **A483**, 371 (1988).
[37] W.D. Myers, W.J. Swiatecki, T. Kodama, L.J. El-Jaick, and E.R. Hilf, Phys. Rev. C **15**, 2032 (1977).
[38] A.J. Sierk, Phys. Rev. C **33**, 2039 (1986).
[39] Lev. D. Landau, Evgenij M. Lifšits, and Lev. P. Pitaevesky, *Fisica Statistica* (Editori Riuniti, Roma, 1986).
[40] D. Neuhauser and S.E. Koonin, Nucl. Phys. **A462**, 163 (1987).
[41] A. Bonasera and F. Gulminelli, Phys. Rev. C **39**, 1179 (1989).
[42] A. Bonasera, M. Bruno, C.O. Dorso, and P.F. Mastinu, Riv. Nuovo Cimento **23**, 1 (2000) and reference therein.